F-15 ACTIVE Flight Research Program

by
James W. Smolka (M), NASA Dryden Flight Research Center[1]
Laurence A. Walker (F), McDonnell Douglas Aerospace[1]
Major Gregory H. Johnson (M), Air Force Flight Test Center[1]
Gerard S. Schkolnik, NASA Dryden Flight Research Center[2]
Curtis W. Berger, Pratt & Whitney[3]
Timothy R. Conners, NASA Dryden Flight Research Center[4]
John S. Orme, NASA Dryden Flight Research Center[5]
Karla S. Shy, NASA Dryden Flight Research Center[6]
C. Bruce Wood, Pratt & Whitney[7]

Introduction

Thrust vectoring technology has been successfully demonstrated on several previous programs to provide tactical maneuvering advantages in the very slow speed, very high angle-of-attack (AOA) flight regime. This technology has matured to the extent that it is being incorporated into present day fighter aircraft designs. For many years, AV-8 aircraft have employed thrust vectoring during air combat engagements against conventional fighter aircraft. The F-15 Short Takeoff and Landing/Maneuver Technology Demonstrator (S/MTD) research program demonstrated the use of pitch-only thrust vectoring for enhanced pitch maneuvering authority.[1,2] The F-18 High Alpha Research Vehicle (HARV) used pitch and yaw thrust vectoring vanes to explore aerodynamics up to 70 degrees AOA and to perform a limited tactical utility investigation.[3] The X-31 program used pitch and yaw thrust vectoring vanes to perform a more detailed exploration of the tactical utility of this technology during one versus one aircraft engagements against modern U. S. fighters at angles-of-attack up to 70 degrees.[4] The YF-22 used pitch-only thrust vectoring to provide enhanced pitch maneuvering authority at slow speeds.[5] The F-16 Multi-Axis Thrust Vectoring (MATV) program used production representative, axisymmetric thrust vectoring nozzle technology to further explore the tactical utility of thrust vectoring during one versus one and one versus two aircraft engagements against modern U. S. fighters at unlimited

[1] Test Pilots
[2] Chief engineer
[3] P&W Project Manager
[4] Principle propulsion engineer
[5] Principle performance engineer
[6] Principle displays engineer
[7] P&W Principle systems engineer

angles-of-attack.[6] Both the production F-22 and the pre-production JSF (Joint Strike Fighter) aircraft will employ some form of thrust vectoring to enhance maneuverability. Almost all of the thrust vectoring utility explored to date has been concentrated in the low speed, high AOA flight regime. The overall goal of the F-15 Advanced Control Technology for Integrated Vehicles (ACTIVE) test program is to expand the flight envelope in which useful thrust vectoring is available to enhance aircraft performance, maneuverability, and controllability with production-representative nozzles (fig. 1).[7]

Figure 1. The ACTIVE test vehicle.

The current phase of the ACTIVE flight test program contains four objectives designed to evaluate the capabilities and benefits of the Pitch/Yaw Balance Beam Nozzles (P/YBBN): 1) nozzle envelope expansion, 2) nozzle jet effects identification, 3) aircraft and nozzle performance, and 4) Adaptive Aircraft Performance Technology (AdAPT).[8,9] Nozzle envelope expansion is the primary objective of the program and includes functional operability of the convergent and divergent actuation systems and control logic, engine and nozzle compatibility, and vector force model validation. The nozzle jet effects identification explores aircraft response measurements to estimate steady-state and dynamic vectoring forces and moments imparted to the aircraft. The aircraft performance testing evaluates incremental improvements in classical aircraft performance due to the

addition of the P/YBBN; whereas, nozzle performance testing evaluates the nozzle's ability to efficiently vector the engine exhaust. AdAPT optimizes the performance of the complete aircraft and vectoring system in real-time using a generic, adaptive, measurement-based algorithm. Flight test is divided into two phases: nozzle envelope expansion and research. Envelope expansion will clear nozzle operation to 6.5g, 2.0 Mach, 1600 psf dynamic pressure, and 30 degrees angle-of-attack, allowing adequate capability to meet the research requirements.

The F-15 ACTIVE program is managed by the NASA Dryden Flight Research Center located at Edwards Air Force Base, California. The prime contractors for the program are Pratt and Whitney (P&W), a division of United Technologies, West Palm Beach, Florida and McDonnell Douglas Aerospace (MDA), St. Louis, Missouri. Program support is provided by the Air Force Materiel Command through the Wright Laboratories, Dayton, Ohio. Additionally, a technical steering committee consisting of representatives from NASA, the United States Air Force (USAF), P&W, and MDA provides technical oversight and program direction.

The F-15 ACTIVE flight test program is jointly conducted by NASA, USAF, MDA, and P&W. NASA provides engineering and technical support, data measurement, recording, analysis, and aircraft maintenance. MDA and P&W provide on-site engineering support. USAF provides engineering support. NASA, USAF, and MDA provide test pilot support.

This paper presents a description of the test aircraft, and discussion of flight test techniques. Results gathered from both nozzle envelope expansion and nozzle performance tests during ground and flight operations will be presented.

Test Aircraft Description

The test aircraft, NASA 837, is pre-production F-15B number 1, (USAF S/N 71-0290) on loan to NASA from the Air Force. The aircraft was previously used for the F-15 S/MTD program. The aircraft is highly modified and is not representative of production F-15 aircraft. It was selected to serve as the research testbed for the ACTIVE program because of the flexibility of its unique quad-redundant, digital, fly-by-wire, flight and propulsion control system. Figure 2 summarizes the flight test configuration of the aircraft.

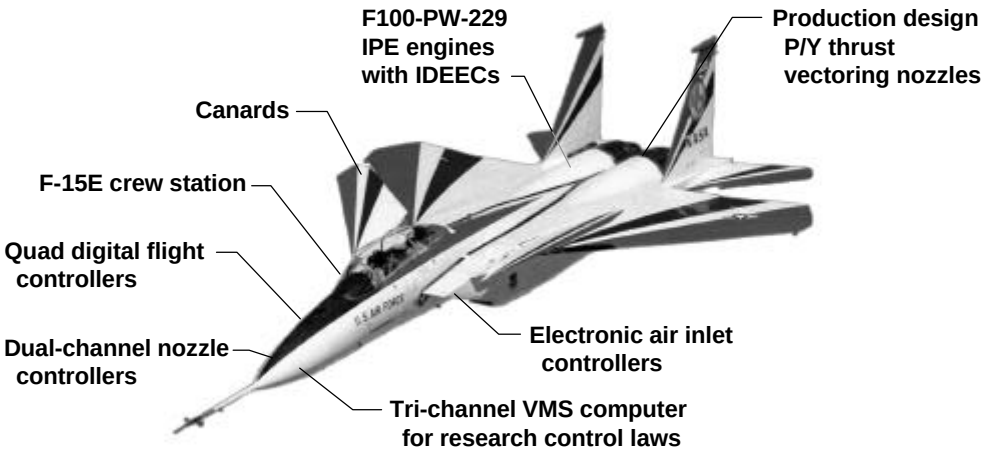

Figure 2. The ACTIVE vehicle configuration.

Aircraft Modifications

External modifications to the aircraft included two canards mounted on the upper inlet area forward of the wing. The canards are modified F-18 horizontal tail surfaces. Additionally, the aircraft is equipped with a flight test nose boom configured with angle-of-attack and sideslip vanes and a total temperature probe.

The aircraft is equipped with two F100-PW-229 turbofan engines modified with axisymmetric P/YBBNs which can vector up to 20 degrees off of the nominal engine thrust line in any direction. An asymmetric thrust departure prevention system (ATDPS) was incorporated into the FC control laws to enhance safety in the event of engine malfunctions at supersonic Mach numbers. A more detailed description of the engines and nozzles is presented below in the **Propulsion System Description** section of this paper.

The aircraft structure has been modified to accommodate 4,000 pounds of lateral vectoring force. Structural modification made previously in conjunction with the S/MTD program for pitch vectoring were retained. Pitch vectoring structural load limits were 6,000 pounds, but vector forces are limited to 4,000 pounds for the ACTIVE program. The aircraft skin contour and structure in the aft fuselage area were modified to accommodate the larger size of the vectoring nozzle actuation system and to provide clearance for full 20 degree yaw vectoring.

The aircraft is controlled via a quad-redundant, digital, fly-by-wire, flight control (FC) system. All mechanical linkages between the control stick, rudder

pedals, and control surfaces have been removed from the aircraft. The throttles digitally control the engines through the FC, 1553 MUX bus, and Improved Digital Electronic Engine Controllers (IDEECs). No mechanical linkage exists between the throttles and the engines.

The aircraft cockpit has been reconfigured to closely resemble the F-15E cockpit. A control panel for the instrumentation system replaces the center multi-purpose color display (MPCD) in the front cockpit. Additionally, unique flight test pages have been added to the multi-purpose display (MPD) options available for selection by the pilot. Two flight test displays, the Dial-A-Gain (DAG) display and the ACTIVE display, are especially noteworthy with respect to the test described in this paper. The DAG display allows the pilot to select 1 of 15 DAG sets. The DAG system functions primarily to establish software test limits for the research control law commands from the Vehicle Management System Computer (VMSC). DAG parameters include: pitch or yaw thrust vectoring force limits, test maneuver load factor limits, test maneuver AOA limits, trim authority limits to the various aerodynamic surfaces, disabling of roll to yaw crossfeeds, and disabling of inner loop control system aileron or differential canard commands. DAG set parameter tables are preprogrammed into the FC and are fixed for the duration of a flight test phase. The ACTIVE display allows the pilot to select 1 of 15 datasets stored in the VMSC. The ACTIVE dataset architecture is highly capable and flexible. Encoded in the ACTIVE dataset is the selection of: 1) either the Programmable Test Input (PTI) or AdAPT research control law mode, 2) aerodynamic or propulsion control effector commands, 3) excitation waveform characteristics such as piecewise linear and/or sinusoidal, effector amplitudes, frequencies and durations. Each load of 15 ACTIVE datasets can be easily reprogrammed between flights to accommodate entirely different test requirements.

The Integrated Flight/Propulsion Control System (IFPC) has been augmented from its original S/MTD configuration by adding the VMSC. The VMSC performs computationally intensive outer loop control functions, such as performance optimization for the AdAPT tests. In addition to the VMSC, four other computers are integrated with the FC: two (left and right) Electronic Air Inlet Controllers (EAIC) and two IDEECs for the F100-PW-229 engines. The ten separate computers forming the ACTIVE flight control system are fully integrated using 1553 multiplex data buses (fig. 3). This architecture allows VMSC resident algorithms to schedule the pitch and yaw vectoring, to trim all aerodynamic surfaces (individually and in any combination), to modify the scheduling of the air inlets, and to modify the operation of the engines. Thus, all aerodynamic and propulsion control effectors are accessed by the VMSC, allowing them to be integrated for maximum performance.

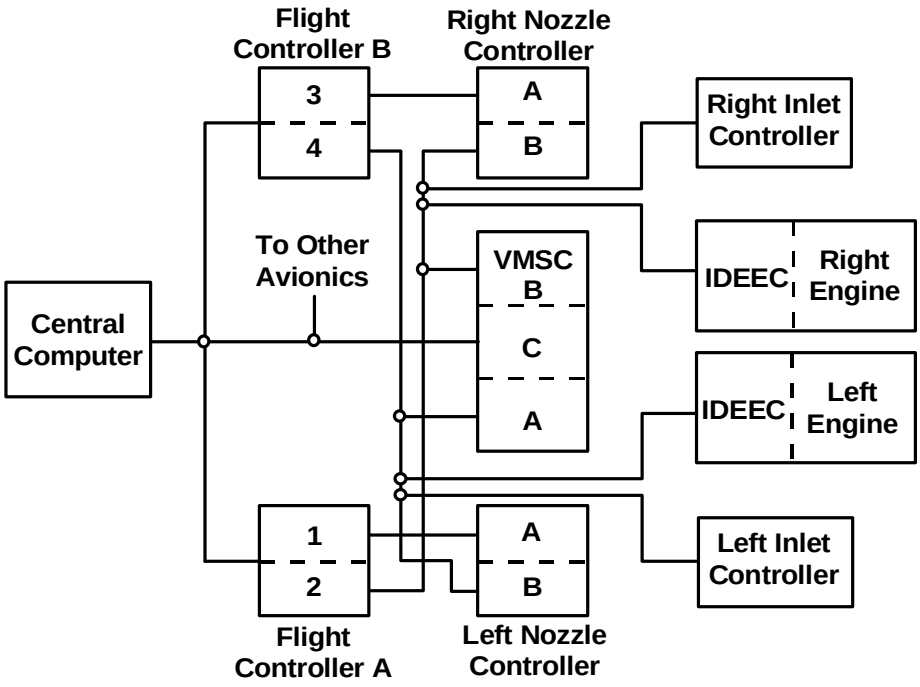

Figure 3. The ACTIVE flight control system computer architecture.

The aircraft is configured with a pre-production hydraulic system. The system differs from production F-15B aircraft in that the wing flaps and ailerons are powered by utility hydraulics only. The aircraft utility hydraulic system was modified by splitting the production utility system, with its two interconnected flow paths, single reservoir and redundant hydraulic pumps (one driven by each engine) into two distinct systems with two totally independent flow paths, separate reservoirs and non-redundant hydraulic pumps (each driven by only one engine). This insured that an actuator failure in one of the thrust vectoring nozzles would not result in a complete loss of the utility hydraulic system. Additionally, the left utility system provides power for all of the systems in the production utility A circuit plus recharging for both Jet Fuel Starter (JFS) accumulators. The only common connection between the utility systems is at the emergency generator. A priority valve selects which utility system powers the emergency generator.

Flying Qualities

The F-15 ACTIVE flying qualities are significantly improved over production F-15 aircraft. Aircraft response is crisp and heavily damped throughout the research flight envelope. Subsonic roll rates are slightly reduced from production aircraft, but are still about 200 degrees per second at most flight conditions. In supersonic conditions, roll rates are higher than production aircraft. Roll coordination at all conditions is superior than production aircraft. Directional stability is enhanced by the canards and is approximately twice that of production

aircraft at Mach 2.0. Stick forces in the landing pattern are somewhat higher than normal and there is a slight nose down rotation at touchdown to facilitate derotation for its former thrust reversing capability. These features are left over from the F-15 S/MTD program, where they were incorporated to facilitate short field landings.

In-flight refueling is restricted to the KC-135 aircraft only using a test boom operator due to the limited clearance between the refueling boom and the left canard. In the refueling configuration, the canards are biased 8 degrees trailing edge down to provide increased clearance from the boom. The aircraft is typically refueled with the boom more extended than normal, with reduced lateral error tolerance, and lower than normal in elevation. Despite the limited refueling envelope, all the pilots agree that the aircraft has excellent handling qualities. Positional control on the boom is superb.

Figure 4. F100-PW-229 engine installation in the ACTIVE aircraft.

ACTIVE Propulsion System Description

The ACTIVE propulsion system consists of two F100-PW-229 engines (fig. 4), each of which is equipped with a P&W axisymmetric thrust vectoring P/YBBN featuring independent exit area control (fig. 5). An engine mounted IDEEC and avionics bay-mounted Nozzle Controller (NC) provide closed-loop control of each respective component. The VMSC allows the pilot to select vector data sets for execution in the NC via the FC. Figure 6 presents a schematic of ACTIVE's nozzle system architecture.

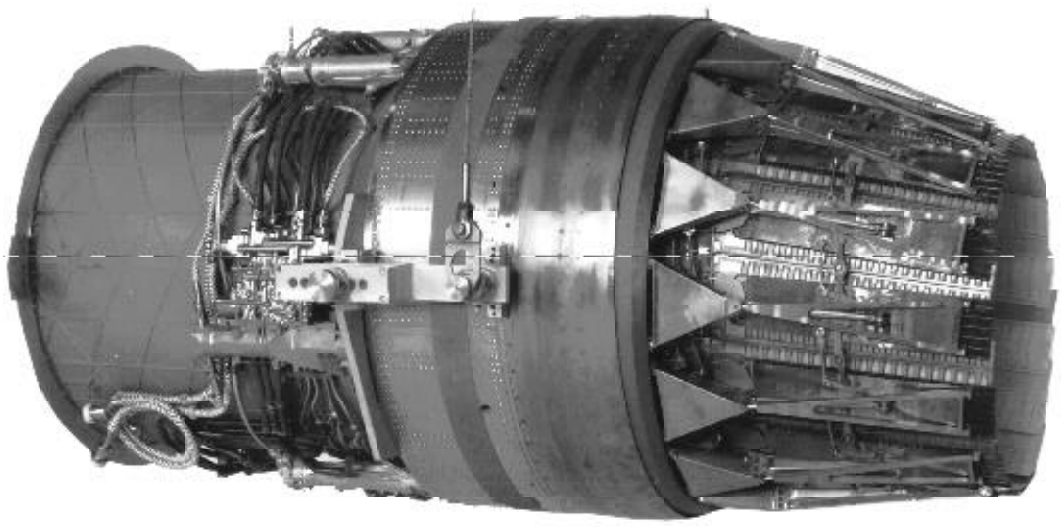

Figure 5. Pitch/yaw balanced beam nozzle module.

F100-PW-229 Engine

The F100-PW-229 is the most recent production model in the F100 series of engines. It is an augmented 29,000 lbf thrust class motor, featuring a three stage fan and ten stage compressor, each driven by a two stage turbine. An eleven segment fuel delivery system within the augmentor delivers smooth afterburner light-off and transient performance.

A small number of modifications to the main body of the engine were required to support the addition of the vectoring nozzle (fig. 7). These included strengthening the augmentor duct and front and rear fan ducts to accommodate the off-axial loads generated during vectoring. Minor rerouting and repositioning of external hardware on the augmentor duct as well as an increase in the static structure diameter was required to provide clearance for the nozzle's divergent actuation system.

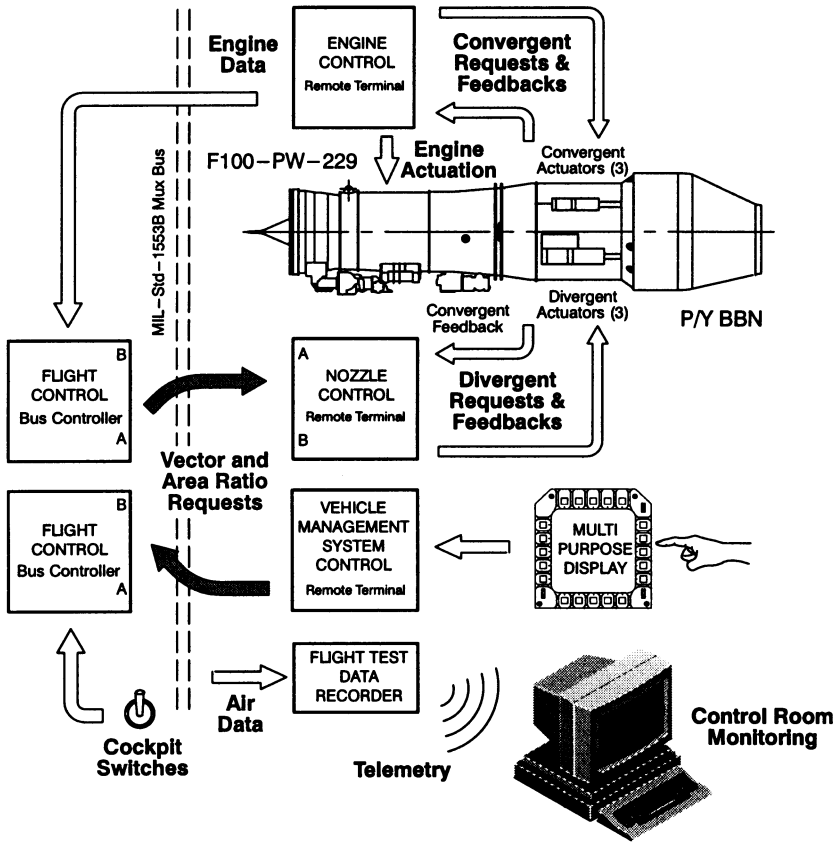

Figure 6. P/YBBN actuation and control system architecture.

Both the Bill-Of-Material (BOM) and P/YBBN convergent nozzle sections are pneumatically powered by engine bleed air. Two of the five BOM convergent actuators were removed to provide clearance for the divergent actuation system. Consequently, the remaining three actuators were load-limit scaled to five-thirds their original BOM design. Though larger in size, they are identical in form and function to the BOM actuators. Because the convergent section loads remained virtually unchanged relative to a BOM nozzle, no significant redesign of its pneumatic drive system or internal structure was required.

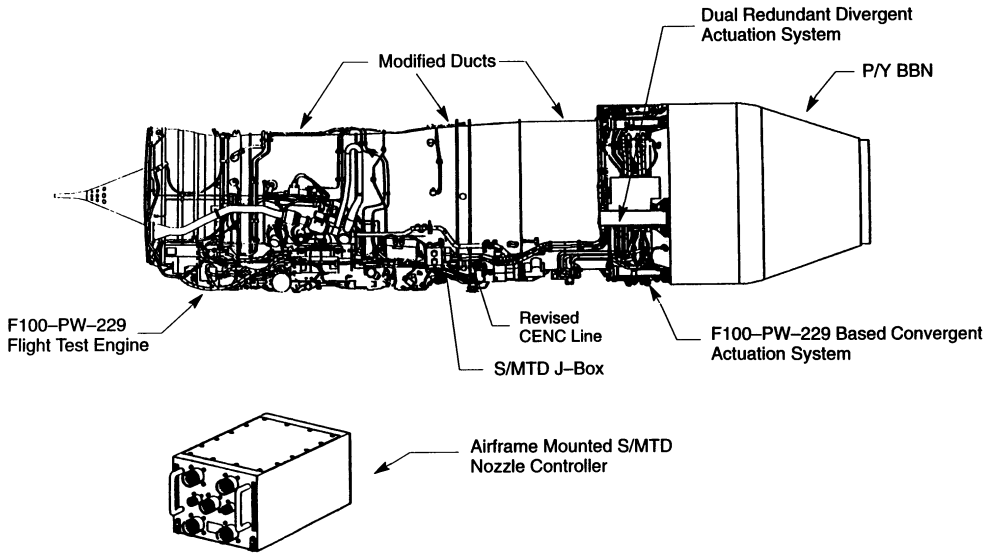

Figure 7. Engine modifications required to support the P/YBBN.

Engine Control

A full-authority IDEEC provides the pilot with unrestricted throttle movement throughout the flight envelope while maintaining engine operation within limits. A hydro-mechanical secondary engine control (SEC) provides get-home capability in the event that the IDEEC becomes unable to adequately control the engine. No modifications to the IDEEC hardware were required for ACTIVE; the only software modifications were to establish communication with the aircraft MUX bus.

The IDEEC maintains full, independent control of the nozzle's convergent throat area (A_j), even in the P/YBBN configuration. There is no loss of engine functionality, operational capability, or modification of fault accommodation due to the addition of the vectoring system.

Pitch/Yaw Balanced Beam Nozzle

Nozzle Design

The P/YBBN design was derived from the fleet-proven F100 Balanced Beam Nozzle (BBN), which takes its name from a pressure-balanced flap arrangement that significantly reduces actuation and structural loads relative to an unbalanced system. At a macro level, only three functional additions to the BOM

nozzle were required to allow vectoring capability: 1) a three actuator divergent section actuation system, 2) an annular synchronization (sync) ring to which the divergent actuators, flaps, and link hardware are attached, and 3) additional static structure used to support and enclose the sync ring.

Torsional freedom built into the P/YBBN divergent seal design permits the nozzle to maintain a tight gas path seal. This allows the P/YBBN to maintain thrust coefficient performance identical to a Bill-Of-Material nozzle while non-vectored and provides freedom from flow instabilities while minimizing thrust coefficient loss while vectored.

The majority of the hardware forward of the throat is common to the BOM nozzle while the hardware aft of the throat is derived from the BOM design. The convergent section maintains its mechanical independence from the divergent section. The part count of the production P/YBBN has actually been reduced relative to the BOM nozzle. Most of the sub-system elements of the P/YBBN are flight-line replaceable.

Nozzle Capabilities

The P/YBBN provides up to 20 degrees of mechanical vector angle in any circumferential direction. The mechanical angle is not restricted by engine power setting. The nozzle is, however, subject to a 4000 pound vector force nozzle design limitation which may limit the commanded vector angle.

The nozzle is capable of vectoring at a minimum rate of 60 degrees/second over the entire flight envelope to a maximum rate in excess of 120 degrees/second at certain flight conditions. Vector rate capability has been software limited from 20 degrees/second at high dynamic pressure flight conditions to 80 degrees/second throughout most of the subsonic envelope. Rate limiting simplifies aircraft system safety by protecting against excessive application of vector-produced moments possible with the P/YBBN.

Independent control of the nozzle exit area allows the nozzle exit-to-throat area ratio to be optimized for performance. The Bill-Of-Material divergent nozzle section uses a mechanical linkage system that tracks throat area and pressure loads, but is not capable of independent exit area modulation. Like the BOM nozzle, the P/YBBN divergent section mechanically responds to convergent area modulation, and no divergent actuation is required to set exit area. However, to maintain more optimal nozzle thrust relative to the BOM nozzle, the three divergent actuators are translated collectively in coordination with the convergent modulation to produce changes in the required scheduled area ratio (fig. 8). Vectoring is achieved by differential translation of the three actuators. The

actuator motions required to set exit area and thrust vector angle may be superimposed over each other.

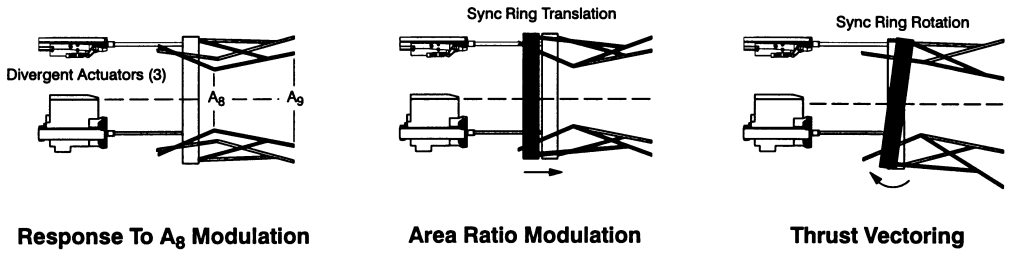

Figure 8. Divergent section motion is dependent upon sync ring position.

Nozzle Actuation

The P/YBBN divergent section is powered by airframe-supplied hydraulics, independent of the convergent section actuation system. For redundancy, each nozzle has been designed to accommodate up to two independent hydraulic sources, although for ACTIVE, only a single utility source is used per nozzle. The aircraft's Utility 1 system drives the left nozzle's divergent actuators, while Utility 2 powers the right nozzle's actuators. Each utility supply line bifurcates into the associated nozzle's dual-line system at the nozzle/aircraft interface.

Within each actuator assembly, redundant electro-hydraulic servovalve (EHSV) torque motors position a main control valve that meters the hydraulic power required to position the actuator based on commands from the Nozzle Controller. A solenoid-driven transfer valve allows selection of a torque motor by way of an electrical command from the NC. A second set of transfer valves is used to lock the actuators into a midstroke position as a last level of fault accommodation, geometrically configuring the P/YBBN to resemble the BOM nozzle when its transfer solenoids are not powered.

Each actuator piston rod contains a dual-wound Linear Variable Differential Transformer (LVDT) providing position feedback information for actuator loop closure in the NC. LVDTs were also added to the Main Control Valve to provide extremely fast fault detection capability in the event of a servovalve failure.

Nozzle Control Computer and Control Algorithm

A dedicated dual-channel Nozzle Control computer is used for closed-loop positioning of the divergent section of each nozzle. The NC uses a multiprocessor configuration in each channel, with one high speed processor dedicated to

managing input/output and fault detection, and the other processor dedicated to control law and fault accommodation functions.

The Flight Control transfers vectoring and area ratio modulation commands over the MUX Bus to the NC, which performs extensive fault detection and accommodation, safely scheduling the divergent actuators in response to the functional requests. Redundancy in the controller and actuation system allows the NC to provide fail-op capability despite the loss of a single NC channel and certain hardware components.

The NC applies software limitations to the vector and area ratio scheduling to maintain the functional integrity of the divergent section mechanism (fig. 9). These kinematic limits prevent the divergent flaps and seals from pulling apart, bunching together or colliding with the other nozzle. The NC also prevents the exit area from becoming smaller than the convergent throat area, which would otherwise cause an unpredictable and potentially damaging shift in the aerothermodynamic operation of the nozzle.

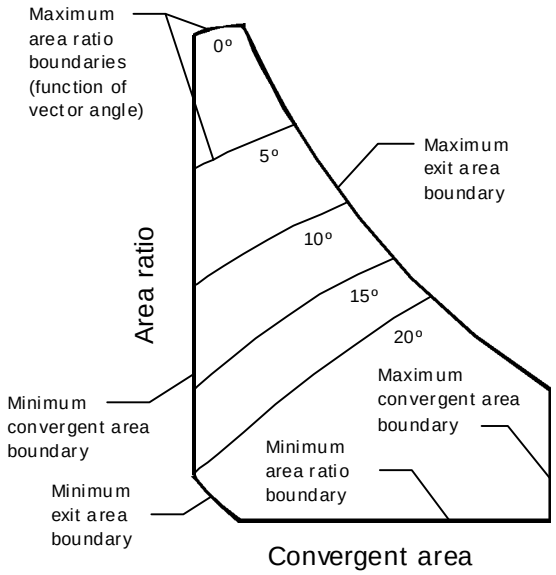

Figure 9. Kinematic envelope of the P/YBBN.

To protect the aircraft, engine and nozzle structure from overload, the NC actively limits vector force to an estimated 4000 lbf per nozzle. An algorithm in the NC predicts engine gross thrust by way of a pressure-area calculation, using sensor supplied data. This gross thrust estimate is used to calculate direct jet vector force based on an average nozzle flap vector angle. Second, an estimate is made by the NC of the force differential created by internal flow effects (nozzle induced force) that can either reduce or additionally turn the thrust vector. Third, an estimate is made of the external aerodynamic lift force that the divergent section imparts to the aircraft while vectored. The three components are summed together as a total

vector force (fig 10). If the NC estimates that a commanded vector angle request will result in a vector force exceeding 4000 lbf, it will limit the angle to prevent exceeding this value. In addition, the FC may further limit the commanded vector angle in order to prevent aircraft departure.

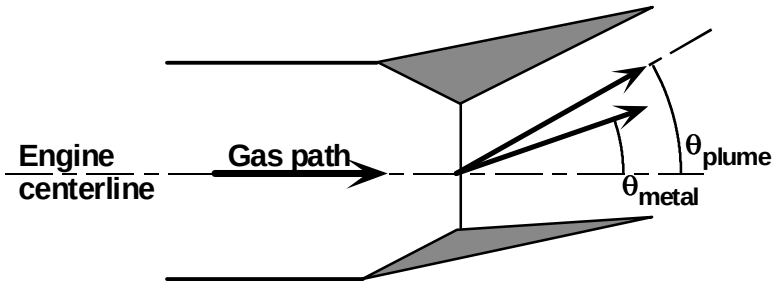

(a) Nozzle vector angle definitions.

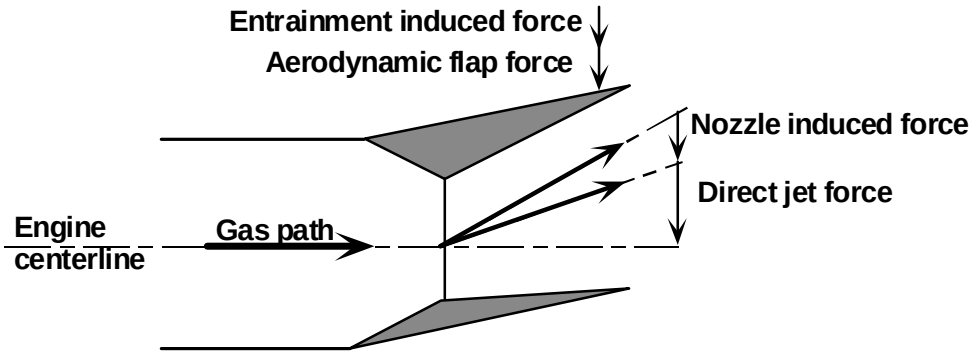

(b) Nozzle vector force components.

Figure 10. Nozzle vector angle definitions and vector force components.

The NC also limits vector and area ratio requests to the load-carrying capability of the divergent actuators. The algorithm limits maximum vector angle and the amount of area ratio modulation below optimum to ensure that predicted divergent actuator loads are not exceeded. This limiting occurs in the far right-hand side of the flight envelope and only in the augmented power range.

An autonomous Initiated Built-In Test Mode (IBIT) was designed into the NC software to verify actuation system functionality prior to flight, by performing a programmed series of motions and mode transfers. Nozzle Control fault detection and accommodation remains active during these tests, indicating any detected faults.

Inlets

The EAICs maintain schedules for each of ACTIVE's three-surface external compression inlets. Because F100-PW-229 engines are installed in the ACTIVE aircraft, inlet ramp schedules identical to those in the F-15E are used to accommodate the higher airflow requirements of this engine. However, ACTIVE's inlet actuation system hardware is not the same used in the "E" model; this requires special EAIC software to accommodate the actuator stroke-to-ramp angle relationship unique to this aircraft.

Asymmetric Thrust Departure Prevention System

ACTIVE is equipped with an all-software Asymmetric Thrust Departure Prevention System (ATDPS). The ATDPS software resides in the FC and is designed to prevent high speed aircraft departure resulting from asymmetric thrust caused by an engine anomaly. ACTIVE is not susceptible to thrust-induced departure anywhere in its flight envelope while in conventional flight control mode. However, one DAG set designed for specific research tasks reduces the aircraft's directional stability to a degree requiring ATDPS at high speed.

Above Mach 1.1, in the event of an engine fault, the ATDPS sends a MIL power auto-throttle command to both engines and disables any engaged DAG set. This guarantees that the remaining good engine remains under IDEEC control. This is unlike the F-15E's ATDPS system, which commands both engines to SEC mode in the event of a high speed engine fault.

Instrumentation System and Control Room Operations

The aircraft is extensively modified with flight test instrumentation to record digital and analog sensor data to monitor performance, flying qualities, structural loads, 1553 MUX Bus, and propulsion parameters. A total of 3377 parameters are recorded on-board and down-linked to the NASA Dryden Mission Control Center and is available for real-time display. Several specialized displays were developed to allow project engineers to monitor flight data for maneuver quality and flight safety. The most complex and specialized graphics display is the nozzle geometry display (fig. 11). This display was created to monitor nozzle area ratios and vector angles. Two other specialized graphic displays contain vector force and nozzle actuation data, including divergent actuator loads, pitch and yaw internal and external forces, and In-Flight Thrust (IFT) model output.

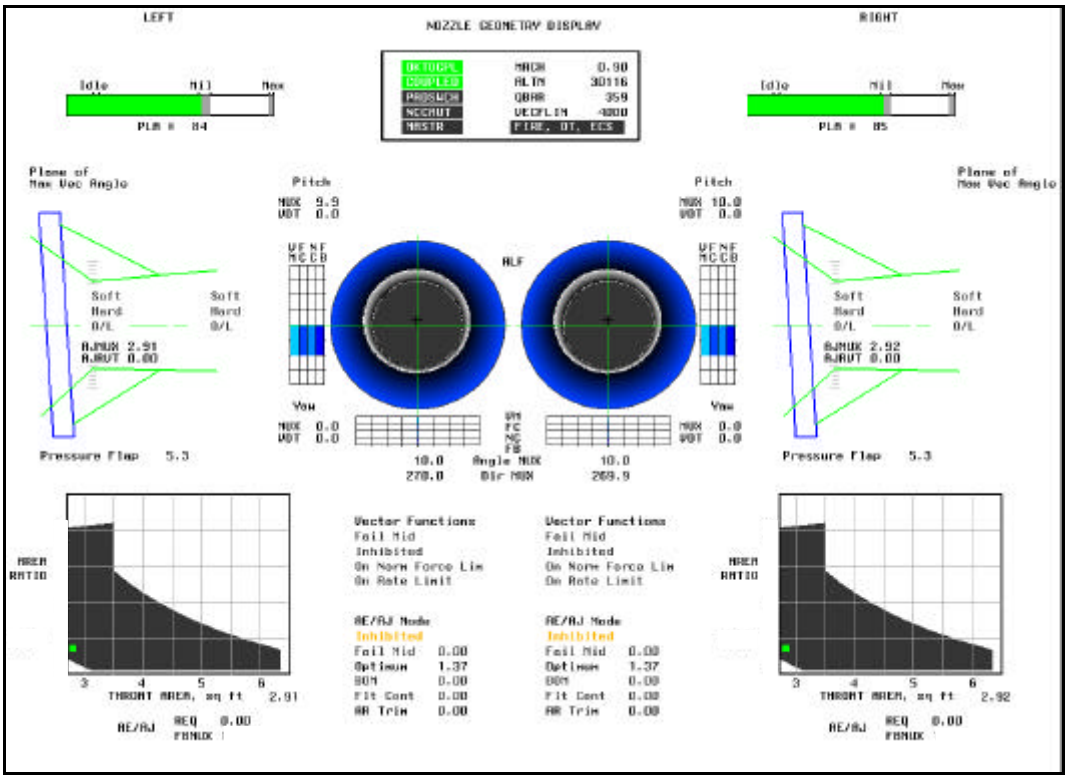

Figure 11. Control room nozzle geometry display.

Ground Test Results

The safe operation and functionality of the vectoring system was validated during extensive ground testing of the F-15 ACTIVE spanning two phases during 1995.

Aft Aircraft Structure Testing

The first phase of ground testing was conducted in June 1995. Prior to testing, the engines were removed, and the aircraft was hard-mounted to the hanger floor using a custom-designed restraint system attaching to the main gear axles and arresting hook mount point (fig. 12).

Figure 12. ACTIVE ground test restraint system.

The purpose of this first test was to verify the capability of the engine mounts and aft aircraft structure to absorb the vector forces, while maintaining adequate stiffness to prevent unacceptable engine deflections. The engine mounts were statically loaded using hydraulic rams and a mock engine plug to emulate thrust and vectoring forces. Simulated vectoring forces up to 110% of the design limit load were applied. This test phase was completed successfully with no structural or deflection anomalies experienced.

A strain gage based measurement system was installed on the engine to measure the forces applied to the aircraft through the engine main mounts, hanger and sway links. This system, used to measure normal and axial forces, was verified and calibrated. The aircraft restraint system was cleared for use for installed engine testing.

Installed Engine Testing

Installed engine demonstration was the focus of the second phase of ground tests and was conducted at the Air Force Flight Test Center's (AFFTC) horizontal thrust stand during November 1995. The primary objectives of this test

were: 1) to verify proper operation of the installed nozzle hardware and control system up to maximum vector rates and loads, 2) to evaluate the accuracy of the on-board thrust model and to quantify nozzle performance, 3) to validate the integrity of the engine mount/aft aircraft structure with dynamic vectoring in the actual thermal and force environment created by the engines, and 4) to verify that engine/nozzle mounted instrumentation met requirements.

Approximately 100 test points were executed in which vector angles, rates and forces were incrementally stepped to their maximum values permitted by the nozzle controllers. Build-up testing was performed in both pitch and yaw directions and at increasingly higher throttle settings up to maximum augmentation. Throttle Bodie sequences at zero-vector angle as well as simultaneous throttle/vector transients were conducted to verify that P/YBBN operation had no adverse affect on engine operability. Proper area ratio scheduling and trim capability were demonstrated as was nozzle transient operation during fail-safe reversion. A vectoring frequency sweep was performed to validate the system's predicted phase and gain margins.

Engine/Nozzle Operability Results

The majority of testing was conducted on the left nozzle because it has the more extensive instrumentation package of the two nozzles. Once demonstrated on the left nozzle, the test end points were repeated on the right. Approximately 260 vector cycles were conducted on both nozzles.

Engine operability was flawless, exhibiting no change in behavior relative to the BOM system. The nozzle system's operation was nearly flawless, with only minor hardware and software modifications required.

The installed ground test environment was predicted to present the most severe thermal operating environment in the P/YBBN operating envelope due to minimal external convective cooling. However, no temperature related problems were encountered with any of the nozzle hardware despite long periods of augmented power vectoring. No thermal damage was experienced by the aircraft's aft structure.

Nozzle Divergent Actuator Loading Results

Hydraulic pressure sensors were installed in each of the chambers of each of the divergent actuators in order to measure the loads applied to the divergent section during axial and vectored operation. Because of the low nozzle pressure ratio conditions of the ground test, the loads were found to be near zero, as expected. When the actuators did experience significant loading, it was usually in

tension, indicating that the divergent flaps were being drawn in toward the gas path.

Engine/Aircraft Structural Results

No engine deflection or mount load limits were exceeded during this test phase, and extensive post-test inspection revealed no stress or damage to the engine mounts, engine–aircraft interfaces or aft aircraft structure.

Flight Test Techniques

Flight testing of the ACTIVE aircraft began with classical, non-vectoring test points for pilot training, safety, and to establish a baseline for follow-on vectoring tests. These included functional check flights, instrumentation checkout, air data calibration, and loads calibration maneuvers. Classical techniques were used to meet these objectives during non-vectoring flight and specific test results will not be fully addressed in this paper.

During thrust vectoring test points, the test pilot established the prescribed flight condition and engaged an ACTIVE dataset to command the proper combination and amplitude of open-loop flight control and vectoring inputs. Many of these datasets lasted five to fifteen seconds, but a few were not complete until well over three minutes. The shorter duration test points were generally "hands off" while some of the longer duration points required low gain pilot inputs to maintain the data band. This modern, programmable approach to open-loop flight testing had the expected advantages of efficient, repeatable test point execution, but posed several challenges and risks to the test team as well. These advantages, challenges, and risks will be detailed below.

Before engaging an ACTIVE dataset, the pilot first selected and engaged a DAG set. Within the DAG set were established limits for flight control and vectoring inputs, normal load factor, AOA, yaw rate and altitude. A lateral load factor limit was coded within the flight control laws to 0.5 g's, and is not selectable. If the aircraft exceeded the selected limits while an ACTIVE dataset was engaged, the flight control system would automatically terminate the dataset and return the aircraft to a non-vectoring baseline configuration. Therefore, the DAG provided a safety net to help prevent aircraft overstress and departure from controlled flight, custom tailored for each research objective. Next, the ACTIVE dataset was selected and engaged for each test point.

The ACTIVE dataset approach proved to have many advantages for this type of open-loop testing. The computerized inputs were crisper and more consistent than was otherwise possible. Additionally, a vast majority of the test

points could not have been accomplished with the controls available to the pilot. Using preprogrammed ACTIVE datasets, engineers could more easily isolate individual flight control and vectoring effects and could often assess these effects real-time in the control room. Finally, this approach decreased pilot workload and allowed the test pilot to concentrate his efforts on test point setup and flight condition maintenance. This made each flight more efficient and produced more consistent and repeatable results.

A risk associated with the ACTIVE dataset approach was the potential for the pilot to select the wrong DAG or ACTIVE dataset. This risk was mitigated by a disciplined protocol between the test pilot and the control room. Strict challenge and response procedures were followed to insure that the pilot was cleared by the control room for DAG or ACTIVE dataset engagements.

Test Procedure Development Using Ground Simulation

Frequently, open-loop testing is considered to be less interesting and less hazardous than the more mission-oriented closed-loop testing. However, the use of ACTIVE datasets had the potential to exceed structural limits during certain open-loop test points. The DAG sets were found to provide inadequate protection for extreme cases. Because of this, the ACTIVE test team developed an exhaustive and systematic approach to evaluate each test point, enabling the team to identify and delete potentially dangerous points from the flight test plan based on results from simulation. The biggest potential problem area occurred during transients resulting from early termination of ACTIVE datasets (by either pilot initiated or automatic disengagement). When the control laws abruptly returned to baseline, the simulator occasional predicted transients exceeding 8 g's. Each test point was flown in the simulator both on and off flight conditions, with nominal completion and pilot commanded disengagement at the worst time, to evaluate trends and determine excessive transient potential.

Flight Test Results

Nozzle envelope expansion was the most critical objective of the ACTIVE program and was accomplished first. All other research required a cleared envelope to evaluate the benefits derived from integrating the vectoring system into the aircraft. Nozzle envelope expansion verified nozzle operability, engine and nozzle compatibility, and evaluated the NC loads model.

Initial flight test results demonstrated the successful operation of the P&W P/YBBN up to Mach 2.0 in non-vectoring flight and up to Mach 1.6 in vectoring operation.

Nozzle expansion was accomplished in classical fashion starting at the heart of the envelope and expanding from there. During testing to date, the nozzle performed flawlessly up to a maximum dynamic pressure of 1500 psf at 32,000 feet at Mach 1.95 (non-vectoring operation) and 950 psf at 10,000 feet at Mach 0.95 (vectoring operation).

During the initial thrust vectoring flights, aircraft response due to thrust vectoring was less than predicted. Additional measurements combined with the aircraft response indicated that vector effectiveness was as much as 50% less than expected.

Engine/Nozzle Operability and Compatibility Results

Nozzle operability testing demonstrated proper operation of the convergent and divergent actuation system and control logic during maximum vector rates, deflections, and loads under steady-state and dynamic conditions. The absence of flow instability or acoustical resonance phenomena was also verified. Proper fail-safe operation of the nozzle was demonstrated throughout the envelope. Finally, the airstart envelope was verified against the BOM F100-PW-229 engine/nozzle envelope.

Engine and nozzle compatibility testing verified that no new stability problems were introduced with the P/YBBNs. This testing demonstrated stall-free operation of the engine under vectoring, maneuvering, and throttle transients.

Nozzle envelope expansion was initiated at 20,000 ft, Mach 0.6. Many of the primary nozzle parameters are a strong function of dynamic pressure, including actuator loads, gross thrust, and nozzle temperatures. Therefore, the expansion's build-up technique primarily followed modest increases in dynamic pressure (no more than a 300 psf increase between conditions) while sweeping through altitude as the expansion progressed into the right side of the flight envelope. In addition, three test conditions were evaluated at dynamic pressures lower than that at 20,000 ft, Mach 0.6 to provide nozzle operational information in the far left side of the envelope. Figure 13 shows the thirteen targeted expansion test conditions in the ACTIVE's flight envelope.

Through flight 20, nine of the thirteen planned expansion conditions have been cleared. Flight 13 was significant in that it demonstrated the highest speed (Mach 1.6) yaw vectoring to date.

Figure 13. Nozzle vectoring expansion envelope.

At each envelope expansion test condition, the left nozzle (containing more instrumentation than the right) was tested through a series of vector doublets that incrementally increased the commanded vector angle in 5 degree increments until the estimated 4000 lbf limit imposed by the nozzle controller was reached. Vector rate was also increased to the maximum allowed by the nozzle controller (varying as a function of flight condition). Once demonstrated in pitch, the sequence was performed in yaw and then the process was repeated again at higher engine settings up to maximum augmentation. Table 1 presents a representative integrated test block. In addition, area ratio modulation was demonstrated throughout the power range by trimming to its maximum and minimum limits about the nominal value. To help ensure that nozzle and aircraft operating limits would not be exceeded, this build-up approach provided the engineers in the control room the opportunity to evaluate force, temperature, aircraft dynamics and engine/nozzle compatibility trends before proceeding to the next build-up test point.

At some flight conditions, additional points were included to demonstrate vectoring with rapidly changing throttle position, vectoring under aircraft loading, and simultaneous pitch/yaw vector commands, among others. Once successfully demonstrated on the left nozzle, the more aggressive test points were then repeated on the right nozzle; otherwise, the right nozzle was cleared by similarity. Once an expansion test sequence was completed, a prescribed region surrounding that condition was then cleared in the sense that no other nozzle demonstration testing was required in that region before performing follow-on research testing using the nozzles.

PLA, deg	Pitch Vector Command, deg	Yaw Vector Command, deg	Vector Rate Command, deg/sec
PLF	±5	0	40
PLF	±10	0	40
PLF	±15	0	40
PLF	±20	0	40
PLF	0	±5	40
PLF	0	±10	40
PLF	0	±15	40
PLF	0	±20	40
PLF	±20	0	80
PLF	0	±20	80
MIL	±5	0	80
MIL	±10	0	80
MIL	±15	0	80
MIL	±20	0	80
MIL	0	±5	80
MIL	0	±10	80
MIL	0	±15	80
MIL	0	±20	80
MAX	±5	0	80
MAX	±10	0	80
MAX	±15	0	80
MAX	0	±5	80
MAX	0	±10	80
MAX	0	±15	80

Table 1. Representative nozzle vector build-up sequence at 20,000 ft, Mach 0.6.

Through flight 20, the nozzles have each acquired over 29.3 hours of flight time. The left nozzle has experienced 1322 vector cycles and 47.4 minutes (9.6 minutes with afterburner) of time-while-vectored whereas the right nozzle has seen 904 cycles and 33.6 minutes (4.1 minutes with afterburner) of time-while-vectored. Each nozzle has experienced nearly 9000 engine power reversals with their attendant throat area modulations and thermal loading cycles.

To date, there have been no nozzle hardware anomalies and no indication of abnormal wear patterns or impending failure of a component. Operating temperatures for both hardware and hydraulics have remained well within safe limits. There have been no nozzle flow instabilities during vectoring, and engine stall margin reduction while vectored has been found to be within acceptable limits at all test conditions.

The nozzle control software has also performed well, providing stable vectoring and area ratio operation throughout the envelope and at all power settings, while always maintaining critical parameters within safe operating limits. As discussed in more detail in the **Performance Results Section**, the data suggest that the nozzle controller is often over-predicting the normal force that it produces at a given vector angle. This over-prediction tends to grow with increasing engine power.

The nozzle controller has performed its force-limiting task as intended. It has never significantly under-predicted vectoring loads, and has always maintained an adequate vectoring load factor of safety. ACTIVE's open-loop vectoring system has allowed the test team to perform additional parametric testing that would otherwise have been impossible with a closed-loop system. For instance, the system has permitted the scheduling of fixed vector angles at off-nominal area ratios to further provide insight into vector force characteristics. The resulting data will be used to redefine the nozzle control scheduling and limiting logic, permitting the nozzle to deliver the full vector force load for which it was designed at all power settings and flight conditions.

The divergent nozzle section actuator loads have matched the predicted values relatively well at MIL power throughout most of the envelope, but have been consistently lower than predicted in the augmented power range. The reduced area ratio schedule in fail-safe mode creates higher actuator loading than at the same flight condition and power setting in the vectoring mode. In the highest dynamic pressure corner of the flight envelope, the non-vectored divergent section actuators were expected to stall against very high loading while in the fail-safe mode. To acquire actual loads data in flight, a test sequence was conducted in which the aircraft climbed and accelerated along a gently increasing dynamic pressure flight path that took it to Mach 1.95 and 32000 ft at MAX power. Figure 14 shows the much lower than predicted forces that were actually experienced during the acceleration at MAX power, contrasted against the close correlation seen during the deceleration at MIL power.

The largest actuation loads were predicted to occur at MAX power. The much lower loads observed during flight testing indicate that the divergent section has a larger than expected margin of safety. This should have significant influence on the final design of a production system, perhaps reducing the weight and cost of the unit.

Nozzle Performance Results

One of ACTIVE's major objectives is the identification of aircraft and nozzle subsystem performance increments due to the addition of the P/YBBN. Trim drag reduction and specific excess power improvements will be assessed by comparing baseline non-vectored vehicle cruise and acceleration performance to that of a P/YBBN-configured vehicle. To increase the reliability of results, analysis techniques necessarily depend upon an accurate estimate of gross thrust, Fg and total vector force, Fv. Ground and flight tests are evaluated for absolute Fg accuracy of both the NC model and the higher fidelity post-flight In-Flight Thrust (IFT) Fg model. In addition, results from evaluating vector effectiveness and area ratio performance are presented.

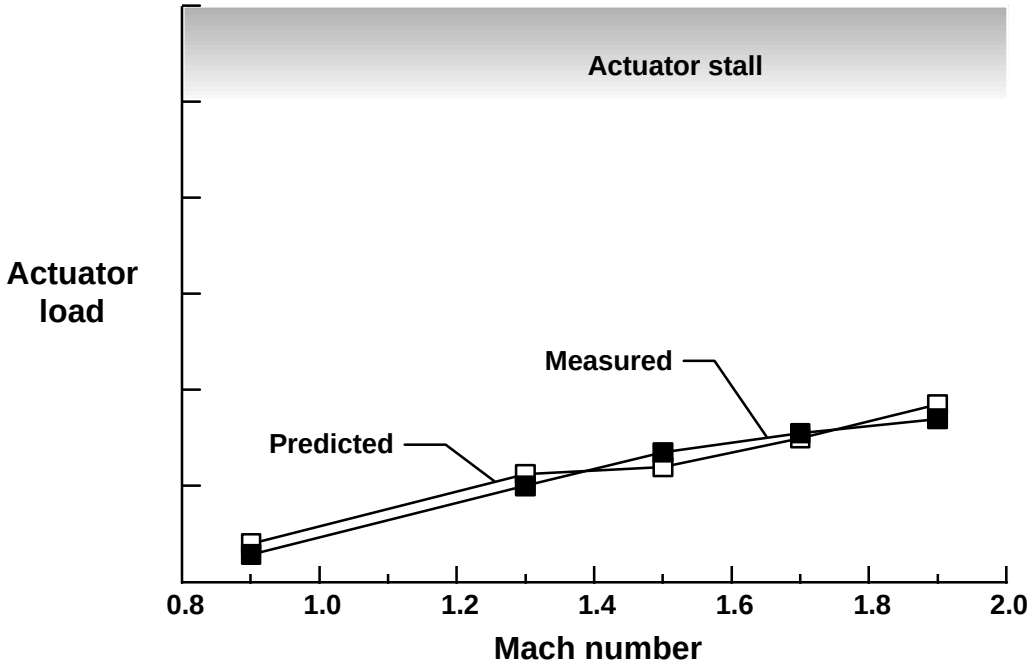

(a) MIL power deceleration results.

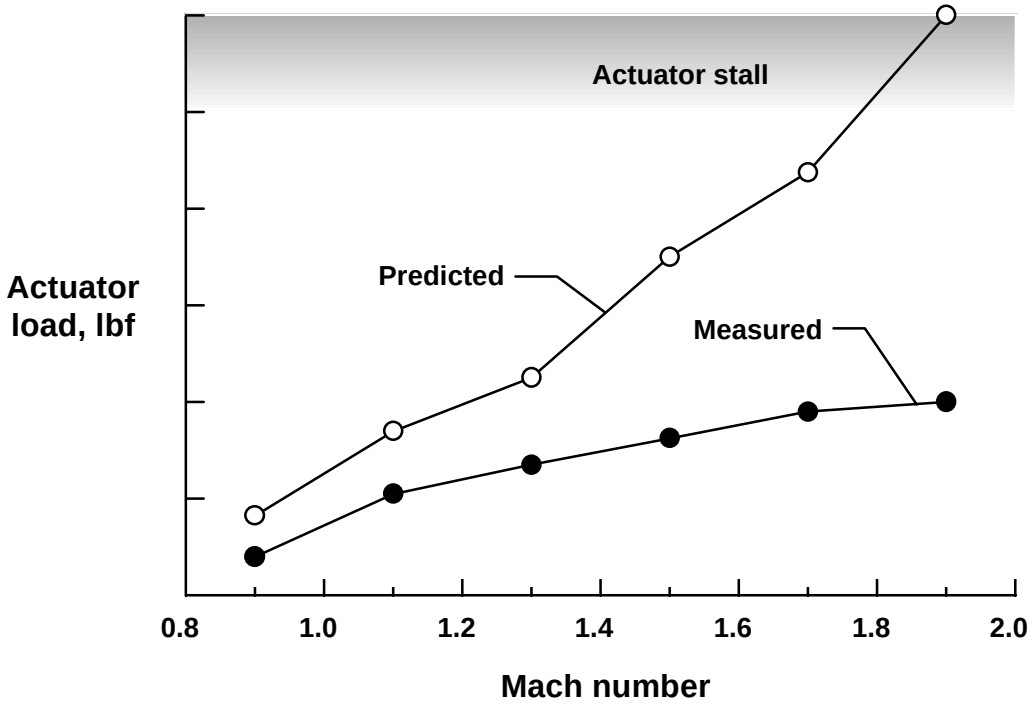

(b) MAX power acceleration results.

Figure 14. Predicted actuator force compared to measured for a non-vectored nozzle in fail-safe mode.

Gross Thrust Evaluation

Gross thrust evaluation was accomplished in two steps. First, results from the installed static engine test provide prediction accuracy relative to thrust stand measurements for both the onboard Nozzle Control (NC) thrust model and the post-flight IFT model. With flight data, comparisons of the NC to the IFT gross thrust predictions provide a second means of assessing modeling accuracy.

The AFFTC horizontal thrust stand has a stated load cell accuracy of ±100 lbf, with systematic error for the ACTIVE aircraft's tie-down configuration most likely adding an additional 100 lbf to 200 lbf to this value. Relative to the accurate benchmark, the NC's gross thrust calculation (Fg_{NC}) was within 2.5 percent at all power settings above Idle. These results indicated no fundamental errors with the onboard model, increasing confidence that the NC would adequately perform its critical vector angle limiting role during flight. The IFT's gross thrust calculation (Fg_{IFT}) was within 1.0 percent at all power settings above Idle. IFT accuracy of this level is excellent for the purposes of post-flight data reduction and standardization. The IFT was then used as the in-flight benchmark to assess the NC gross thrust prediction capability.

Results from ground test and one flight condition, Mach 0.9 at 30000 feet, were analyzed for NC to IFT gross thrust correlation (fig. 15). Overall Fg_{IFT} and Fg_{NC} agree within 2 percent at ground static conditions and within 4 percent at 30000 feet and Mach 0.9. The ground results compare within 1 percent at lower power settings; whereas flight results show reduced correlation at the lower power settings. The best comparison of Fg_{IFT} and Fg_{NC} occurs at MAX power, less than 1 percent. Differences between flight and ground Fg correlation may be attributable to differences in engine pressure ratios.

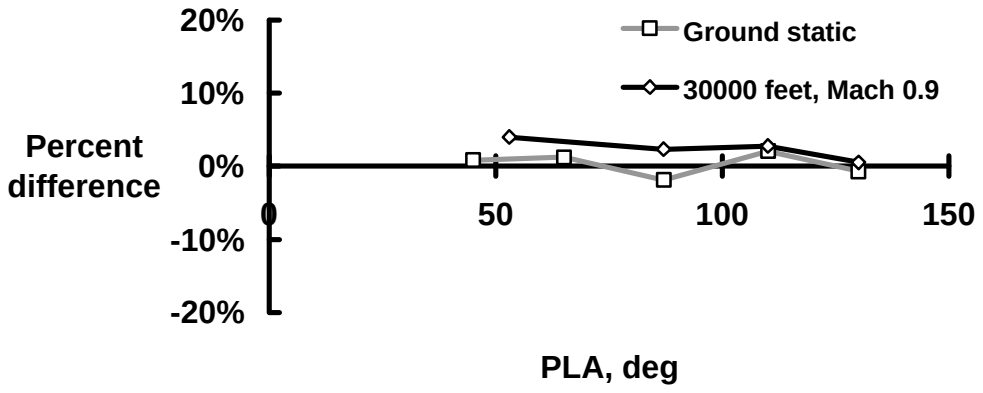

Figure 15. Gross thrust comparison of the nozzle control and in-flight thrust models.

Area Ratio Evaluation

Nozzle performance testing was also conducted to characterize gross thrust sensitivity to nozzle area ratio configuration. The ability to independently modulate area ratio and vector angle offers tremendous flexibility in testing off-scheduled nozzle configurations. The NC schedules an Optimum Area Ratio (OAR) that is designed to yield maximum internal nozzle performance by commanding area ratios that expand the nozzle supply total pressure to ambient pressure. However, it should be noted the static results do not include the effects of external aerodynamic forces on the nozzle.

Baseline ground static results indicate the OAR schedule produces the highest levels of gross thrust of all the area ratios tested (fig. 16). Thrust ratio is defined as the thrust stand load measurement for any given area ratio divided by the stand load measurement at OAR. Figure 16 shows a linear sensitivity of thrust ratio to area ratio for both power settings up to the point where flow separation was encountered. Flow separation was observed to occur for the partial power test at an area ratio of about 1.65. The MIL power results show no signs of flow separation probably because of the higher nozzle pressure ratios (NPRs) at MIL power.

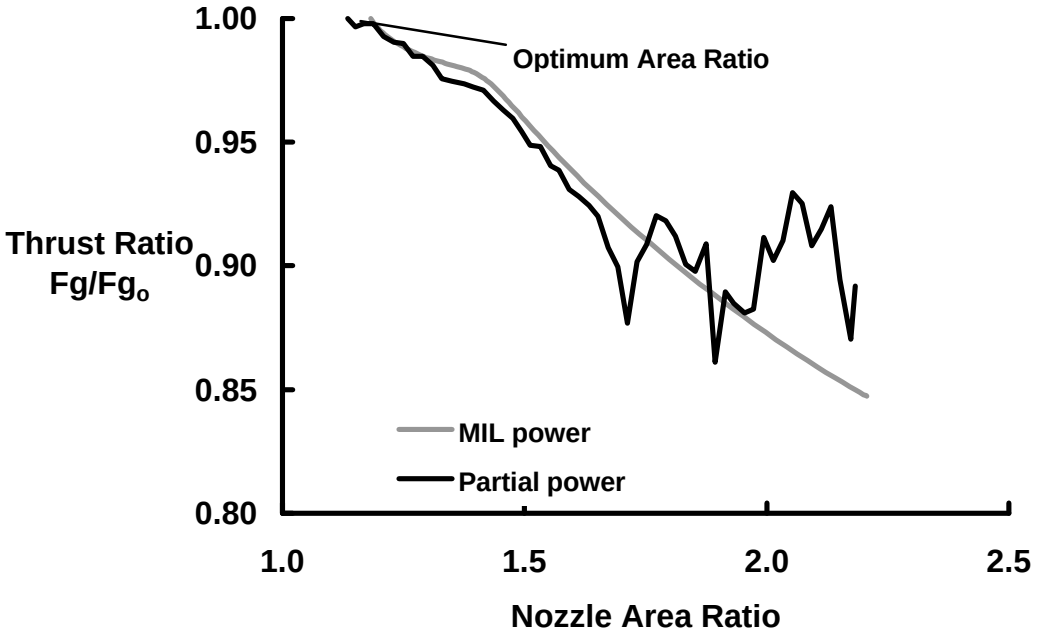

Figure 16. Gross thrust sensitivity to nozzle area ratio during the installed static ground test.

Vector Force Description

As modeled in the NC, the total vector force Fv consists of external and internal force components (fig. 10). Deflecting the nozzle flaps into the free-stream air while vectoring directly generates an aerodynamic flap force. An additional external vector force is induced because of free-stream airflow entrainment about the nozzle that varies with NPR or power setting. The direct aerodynamic flap and the induced entrainment forces comprise the external vector force. Similarly, there exists direct and induced elements of internal vector force. Unlike the aerodynamic flap force, both direct and induced internal forces vary with NPR. The gross thrust acting along the average metal angle is defined as the direct jet force. Because the plume does not exactly follow the metal angle, there also exists a nozzle induced effect force. Possible errors in the identification of nozzle induced effect force are: 1) NC positioning error, 2) surface irregularities of the nozzle walls, 3) aerodynamic losses associated with redirecting momentum such as shock-boundary layer interaction or flow separation, 4) flow leakage, 5) thermal effects, and 6) measurement errors.

All vector and area ratio commands are limited by the NC not to exceed allowable vector force, actuator loads, and kinematic limits. The vector force maximum limit (Fv_{lim}) imposed by the NC is set by the FC DAG up to the P/YBBN designed limit of 4000 pounds. NC-hosted models provide real-time estimates of Fg, Fv, actuator loads. Because of cost and schedule constraints involved with altitude chamber testing, predictions for the vector force and actuator loads were derived from computational fluid dynamics calculations and wind tunnel data. These nozzle load predictions are incorporated into the model with considerable conservatism to ensure adequate loads margin would be encountered throughout flight test. Hence, model conservatism will restrict the nozzle operating envelope and potentially limit the demonstration of full nozzle performance. Flight-test-quantified actual nozzle loads and sensitivities to vector angle, area ratio, and flight condition will permit refinement of these models such that additional performance will be attained.

Vector Effectiveness Evaluation

The effectiveness with which the nozzle exhaust is turned to produce nozzle vector force was evaluated at MIL and MAX power. Two separate data analysis techniques were used to provide insight into vector effectiveness. The first technique compared strain gage derived vector force data against NC predicted total vector force. The second technique compared the estimated exhaust plume angle against the feedback nozzle metal vector angle. The flight-measured vector effectiveness data will lead to refinement of the NC nozzle mechanical scheduling and vector limiting algorithms.

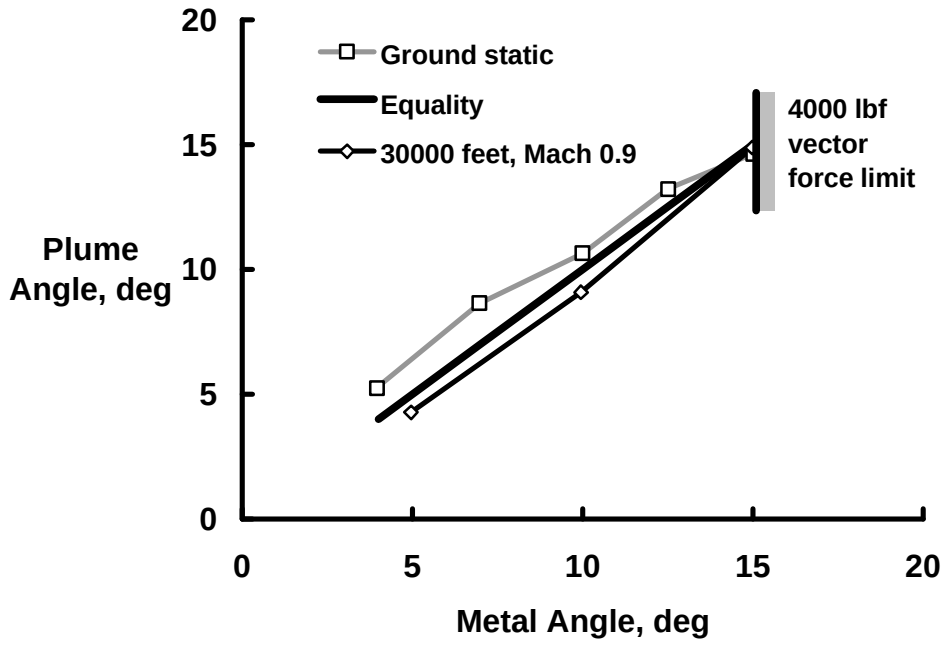

(a) MIL power results.

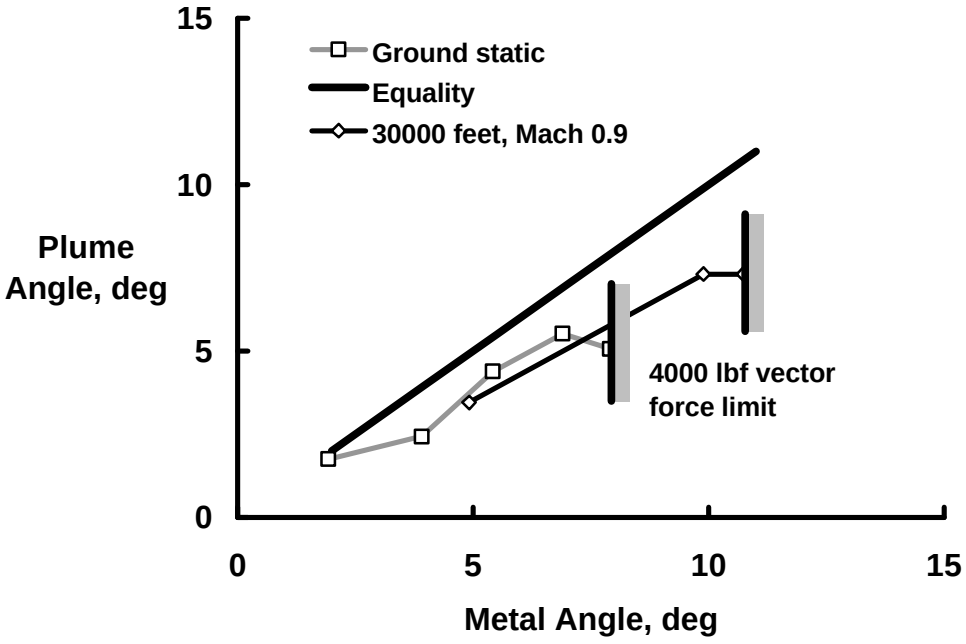

(b) MAX power results.

Figure 17. Vectoring effectiveness at 30000 feet, Mach 0.9.

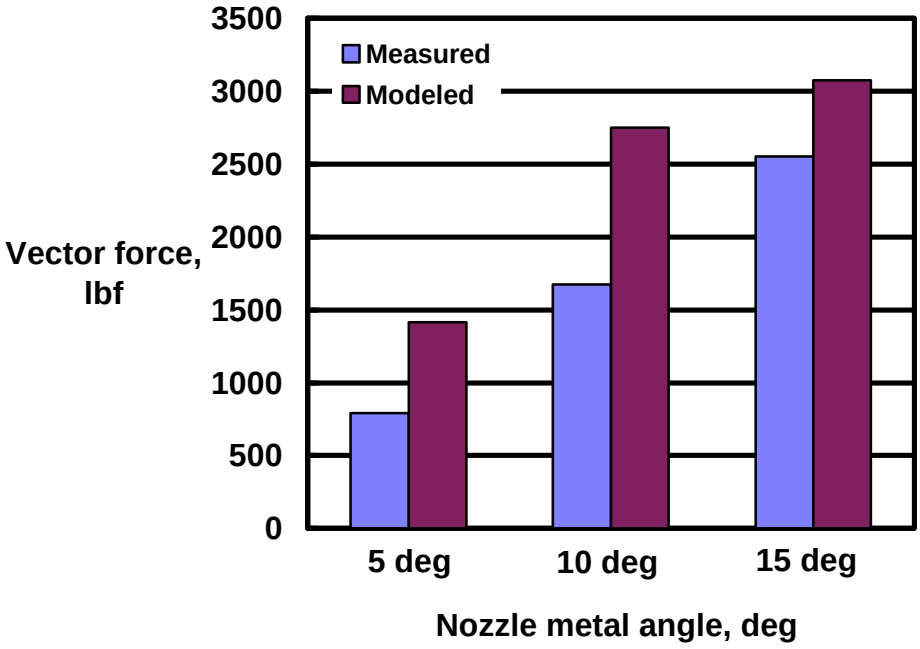

(a) MIL power results.

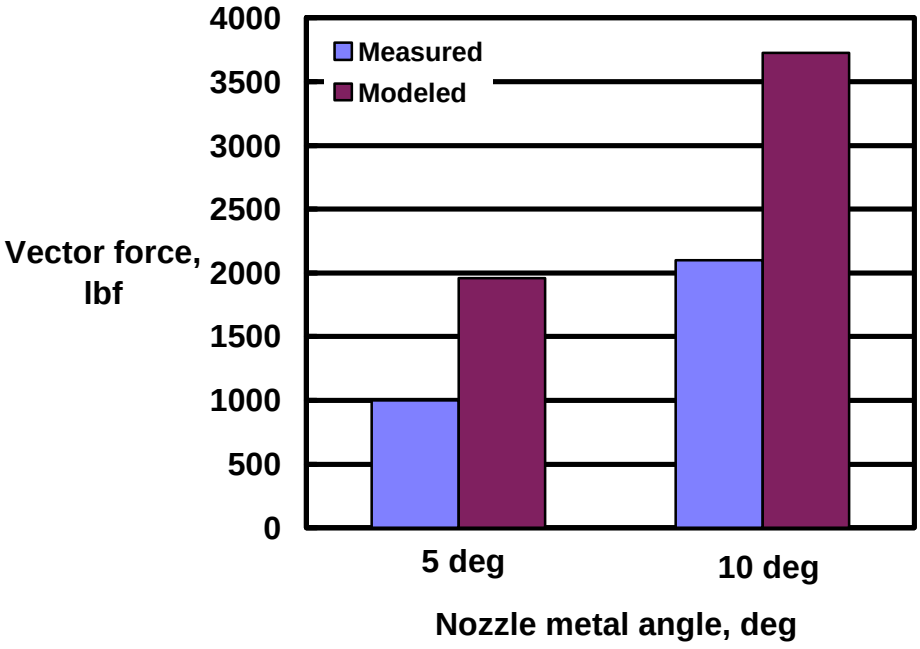

(b) MAX power results.

Figure 18. Vectoring effectiveness at 30000 feet, Mach 0.9.

Findings indicate correlation of metal to plume angle at MIL power was very good and considerably closer than what was observed for the MAX power results. Increased vector effectiveness at MIL power and ground static conditions yields plume angles slightly greater than metal angles (fig. 17). Effectiveness is somewhat less for MIL power flight results. At MAX power, vector effectiveness is greatly diminished and the plume achieves only about 70 to 80 percent of the metal angle at larger vector angles. Thus, vector effectiveness degrades with increased power and in almost all cases plume angles are less than metal angles. The reason for this significant plume-to-metal variation with power is not currently understood and will be further investigated to update the NC models for the purposes of increasing vector effectiveness.

Results from one flight condition, 30000 feet and Mach 0.9, show the NC model underestimates the total vector force by as much as 40 percent at MIL power and 45 percent at MAX power (fig. 18). The vector force analysis reveals discrepancies at MIL power that are not clearly evident from the vector angle analysis. The exaggerated conservatism of the NC vector force model prevents vectoring much beyond 10 degrees at MAX power when there clearly is less than 4000 pounds. In order to test to actual forces of up to 4000 pounds, it may be necessary to raise the model vector force limit greater than 4000 pounds.

Conclusions

All nozzle envelope expansion test points were accomplished successfully and safely, without any significant problems or unanticipated hazards. The P/YBBN developed by Pratt & Whitney is proving to be a successful design for providing modern fighter aircraft with efficient thrust vectoring capability. Additionally, the objective of developing thrust vectoring nozzles that are capable of use as primary flight control effectors appears to be realizable with this design approach.

Several lessons learned during this program are worth noting. First, for an open-loop test program of this nature, accurate ground based simulation was essential to provide the test team with a tool with which to develop flight test techniques. Second, the simulator proved its worth in allowing the test team to identify potential catastrophic test conditions that were not predictable analytically, were unanticipated during the development of the test maneuvers, and for which FC protection logic could not be designed without excessive development time and cost. This underscored the need to collectively weigh software limits, envelope limits, and maneuver restrictions to ensure flight safety. Third, during this type of testing, the rigid engagement protocol developed resulted in no inadvertent inflight engagements of PTI data sets. Fourth, the approach used allowed an efficient and thorough clearance of the nozzle vectoring envelope without any unanticipated transients. And finally, the use of an open-loop approach to the nozzle testing

allowed, for the first time, the quantification of several unique characteristics of axisymmetric thrust vectoring nozzles. Flight testing has revealed a significant discrepancy between what has been measured and modeled for vector effectiveness. The data acquired will be invaluable in the refinement of future closed-loop thrust vectoring designs.

Future Plans

The ACTIVE test program is proving the maturity and reliability of the basic P/YBBN design. Future programs intend to fully integrate the nozzles into the closed-loop control law and to demonstrate performance and handling qualities improvements throughout the current flight envelope. Increased capability, performance and reliability offered by the P/YBBNs will allow expansion into new flight regimes where flight critical thrust vectoring control will be essential.

Acknowledgments

The authors would like to thank Bryan Duke for his contribution in preparing the presentation and the paper. Without his help, we may never have accomplished these tasks in time.

Nomenclature

ACTIVE	Advanced Control Technology for Integrated Vehicles
AdAPT	Adaptive Aircraft Performance Technology
AFFTC	Air Force Flight Test Center
AOA	Angle-of-attack, degrees
ATDPS	Asymmetric Thrust Departure Prevention System
BBN	Balanced Beam Nozzle
BOM	Bill-Of-Material
DAG	Dial-A-Gain
EAIC	Electronic Air Inlet Controller
FC	Flight Control
Fg	Gross Thrust, lbf
Fg_{IFT}	In-Flight Thrust model Gross Thrust, lbf
Fg_{NC}	Nozzle Control Gross Thrust, lbf
Fv	Total Vector Force, lbf
Fv_{lim}	Vector Force Maximum Limit, lbf
HARV	High Alpha Research Vehicle
IBIT	Initiated Built-In Test Mode
IDEEC	Improved Digital Electronic Engine Controller
IFPC	Integrated Flight/Propulsion Control system
IFT	In-Flight Thrust model
IPE	Improved Performance Engine
JFS	Jet Fuel Starter
JSF	Joint Strike Fighter
LVDT	Linear Variable Differential Transformer
MATV	Multi-Axis Thrust Vectoring
MDA	McDonnell Douglas Aerospace, St. Louis , Missouri
MPCD	Multi-Purpose Color Display
MPD	Multi-Purpose Display
MUX	Multiplex
NASA	National Aeronautics and Space Administration
NC	Nozzle Control
NPR	Nozzle Pressure Ratio
OAR	Optimum Area Ratio
P/YBBN	Pitch/Yaw Balanced Beam Nozzle
PTI	Programmable Test Input
P&W	Pratt and Whitney, West Palm Beach, Florida
SEC	Secondary Engine Control
S/MTD	Short Takeoff and Landing/Maneuver Technology Demonstrator
USAF	United States Air Force
VMSC	Vehicle Management System Computer

References

1. McDonnell Aircraft Company, S/MTD Project, *STOL/Maneuver Technology Demonstrator, Volume 1-4, Final Report*, WL-TR-91-3083, September 1991.

2. Crawford, Mark, Brian Hobbs, Steven Roell and Gerard Schkolnik, *STOL/Maneuver Technology Demonstrator Flying Qualities and Integrated Flight/Propulsion Control System Evaluation, Final Report*, AFFTC-TR-91-29, December 1991.

3. Sternberg, Charles A., Ricardo Traven and James B. Lackey, *Navy and the HARV: High Angle of Attack tactical Utility Issues*, N95-14252, July, 1994.

4. Eubanks, David A., Holger Friehmett, Richard Gutter, Richard Haiplik and Quirin Kim, *X-31 Tactical Utility (U), Final Report*, NASA-TM-110455, October, 1995.

5. Barham, Robert W., *Thrust Vector Aided Maneuvering of the YF-22 Advanced Tactical Fighter Prototype*, N94-34610, March 1994.

6. Wilkinson, Todd T., David J. Markstein and Bernard J. Renglli, *MATV/AVEN Flight Test Program, Final Report*, WL-TR-95-3064, June 1995.

7. Doane, Paul, Roger Bursey, and Gerard S. Schkolnik, *F-15 ACTIVE: A Flexible Propulsion Integration Testbed*, AIAA 94-3360, June 1994.

8. Hreha, Mark A., Gerard S. Schkolnik, and John S. Orme, *An Approach to Performance Optimization Using Thrust Vectoring*, AIAA 94-3361, June 1994.

9. Schkolnik, G. S., John S. Orme and Mark A. Hreha, *Flight Test Validation of a Frequency-based System Identification Approach on a F-15 Aircraft*, AIAA 95-2362 and NASA TM 4705, June 1995.